

Ligand Ratio/Solvent-Influenced Syntheses, Crystal Structures, Magnetic Properties of Polydentate Schiff Base Ligand-Dy^{III} Compounds with β -Diketonate Ligand as Co-Ligand

Sheng Zhang,^{*a} Wenjiao Mo,^a Zengqi Zhang,^d Fei Gao,^e Lei Wang,^{*b} Dengwei Hu,^a Sanping Chen^{*c}

^a. College of Chemistry and Chemical Engineering, Baoji University of Arts and Sciences, Baoji 721013, China.

^b. School of Environmental Science and Engineering, Nanjing Tech University, Nanjing 210009, China

^c. Key Laboratory of Synthetic and Natural Functional Molecule Chemistry of Ministry of Education, College of Chemistry and Materials Science, Northwest University, Xi'an, Shaanxi 710069, China

^d. Qingdao Institute of Bioenergy and Bioprocess Technology, Chinese Academy of Sciences, Qingdao 266101, PR China

^e. School of Materials and Metallurgy, Inner Mongolia University of Science and Technology, 7# Alerding Street, Kun District, Baotou 014010, China.

Corresponding authors

Dr. Sheng Zhang, Prof. Lei Wang, Prof. Sanping Chen

E-mail address: zhangsheng19890501@163.com; wlei@njtech.edu.cn;
sanpingchen@126.com

1 The synthesis ligand H₂L

1.1 2-Hydroxy-3-(chloromethyl)-5-methyl-benzaldehyde (HCMB)

HCMB was prepared by a direct chloromethylation of HMB. In a 250 mL round bottom flask, a mixture of 6.4 g (4.7 mmol) of HMB, 7.5 mL of formaldehyde and 25 mL of HCl (12 mol/L) was heated under magnetic stirring to reflux for 15 min. After cool down the reaction to 0 °C, a solid mass was formed in the bottom. The solid was separated from the reaction solution and recrystallized in hot ethanol, yielding 5 g of HCMB (70% yield). The residual solutions were basified with NaOH (pH > 9) prior to discard them. ¹H NMR (400 MHz, CDCl₃) δ 11.24 (s, 1H), 9.80 (s, 1H), 7.42 (d, *J* = 2.1 Hz, 1H), 7.30 (d, *J* = 1.4 Hz, 1H), 4.64 (s, 2H), 2.31 (d, *J* = 4.4 Hz, 3H). ¹H NMR (100 MHz, CDCl₃) δ 196.7, 196.5, 159.5, 157.3, 138.6, 138.1, 134.1, 133.5, 129.3, 129.2, 125.7, 120.4, 120.4, 117.4, 39.9, 20.3, 20.2.

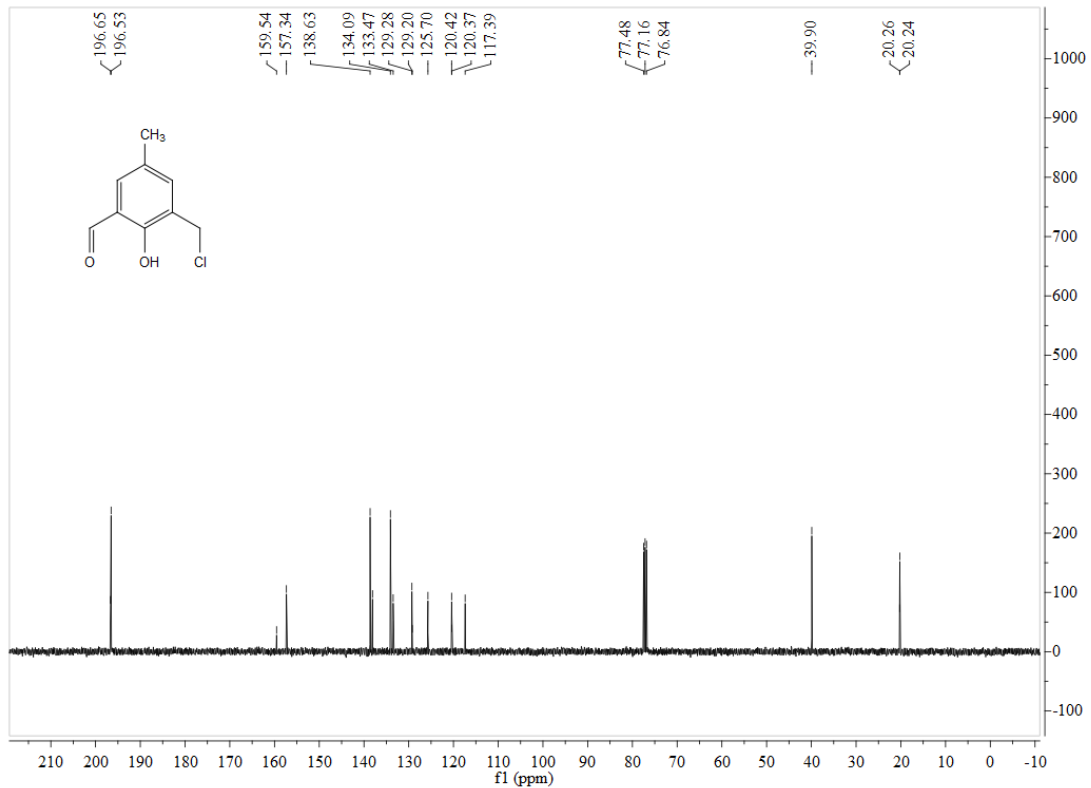


Fig. S1 ¹³C NMR spectra of HCMB.

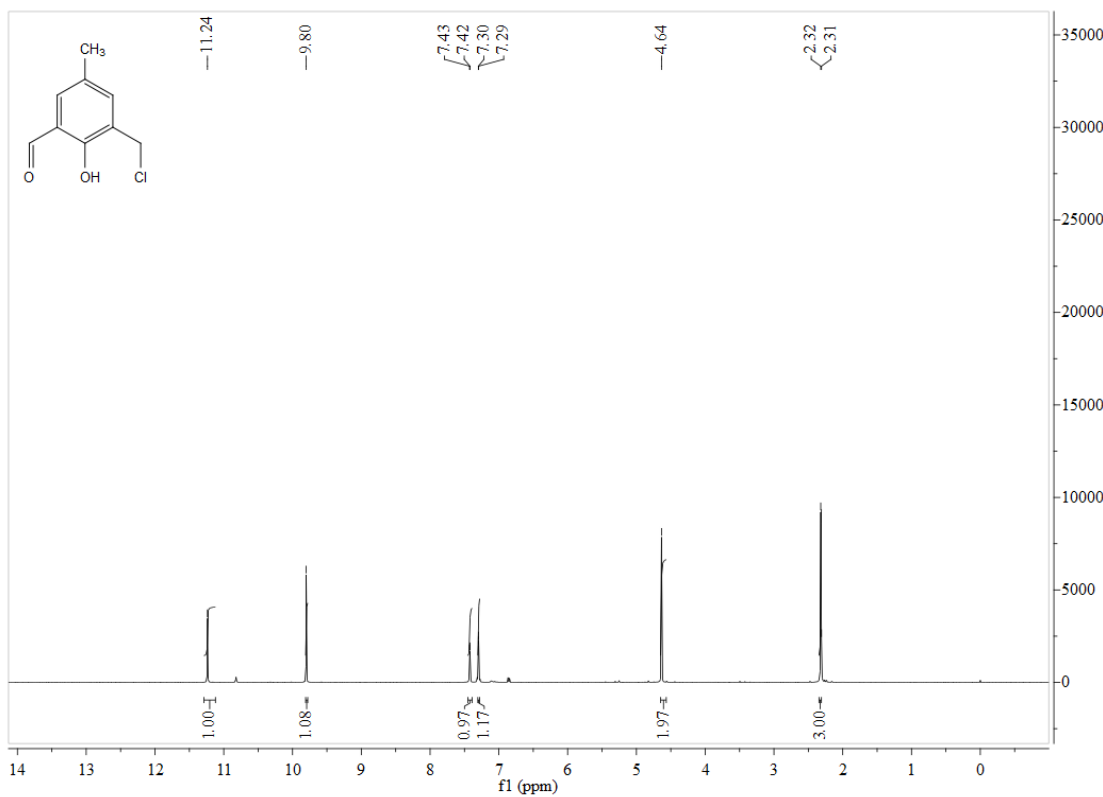


Fig. S2 ^1H NMR spectra of HCMB.

1.2 N,N'-bis(pyridin-2-ylmethyl)ethylenediamine (py₂en)

Py₂en was prepared by a condensation reaction between 2-pyridinecarboxaldehyde and ethylenediamine, followed by reduction with NaBH₄. In a 100 mL round bottom flask, 3.0 mL of pyridine-2-carboxaldehyde (31 mmol) were dissolved in 30 mL of methanol at 0 °C, followed by the addition of 1.0 mL of ethylenediamine (15.5 mmol), under magnetic stirring. After 1 h, 1.2 g of sodium borohydride (31 mmol) was added in small portions and left to react for another 1 h. Then, HCl 6 mol/L was added dropwise up to pH < 2. After removing the solvent, 30 mL of distilled water was added and the pH adjusted to 9–10 with NaOH. The product was extracted with dichloromethane (6 × 50 mL); the organic layers were dried under MgSO₄ and the solvent was removed under vacuum, yielding 2.8 g of a yellow oil of py₂en (85 % yield). ^1H NMR (400 MHz, CDCl₃) δ 8.57–8.51 (m, 2H), 7.62 (td, J = 7.7, 1.8 Hz, 2H), 7.32 (d, J = 7.8 Hz, 2H), 7.14 (ddd, J = 7.4, 4.9, 0.9 Hz, 2H), 3.92 (s, 4H), 2.82 (s, 4H). ^{13}C NMR (100 MHz, CDCl₃) δ 159.8, 149.1, 136.3, 122.1, 121.7, 55.1, 49.0.

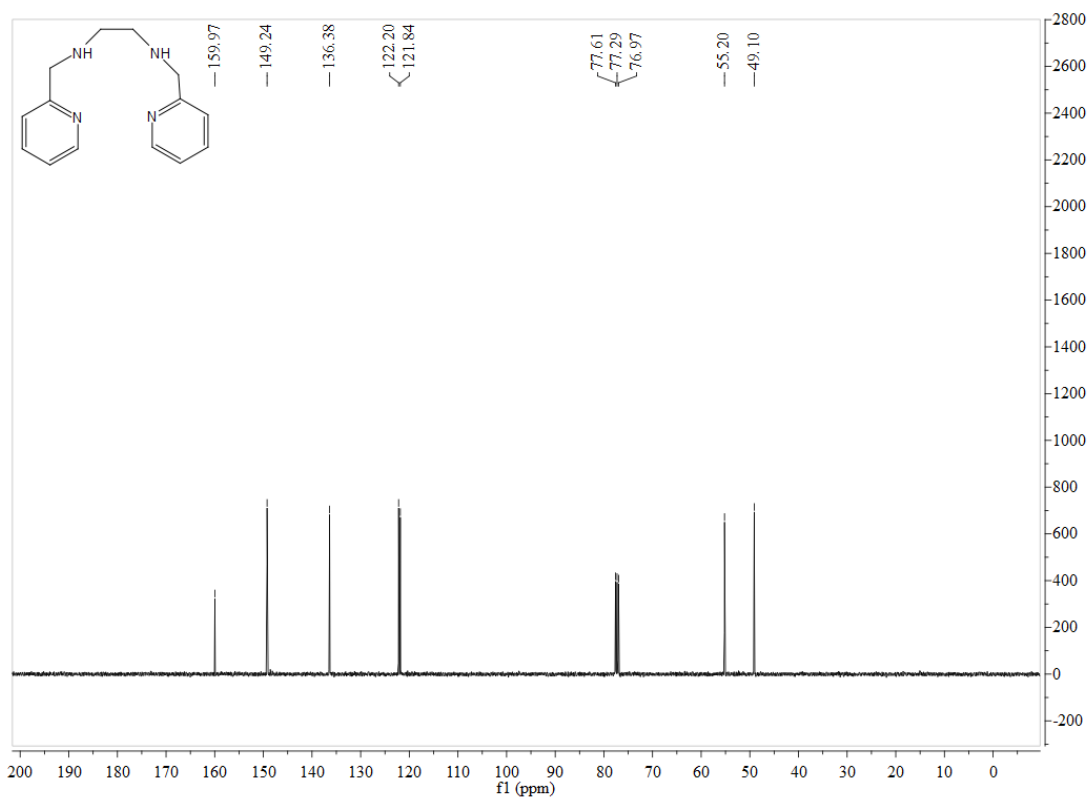


Fig. S3 ¹³C NMR spectra of py2en.

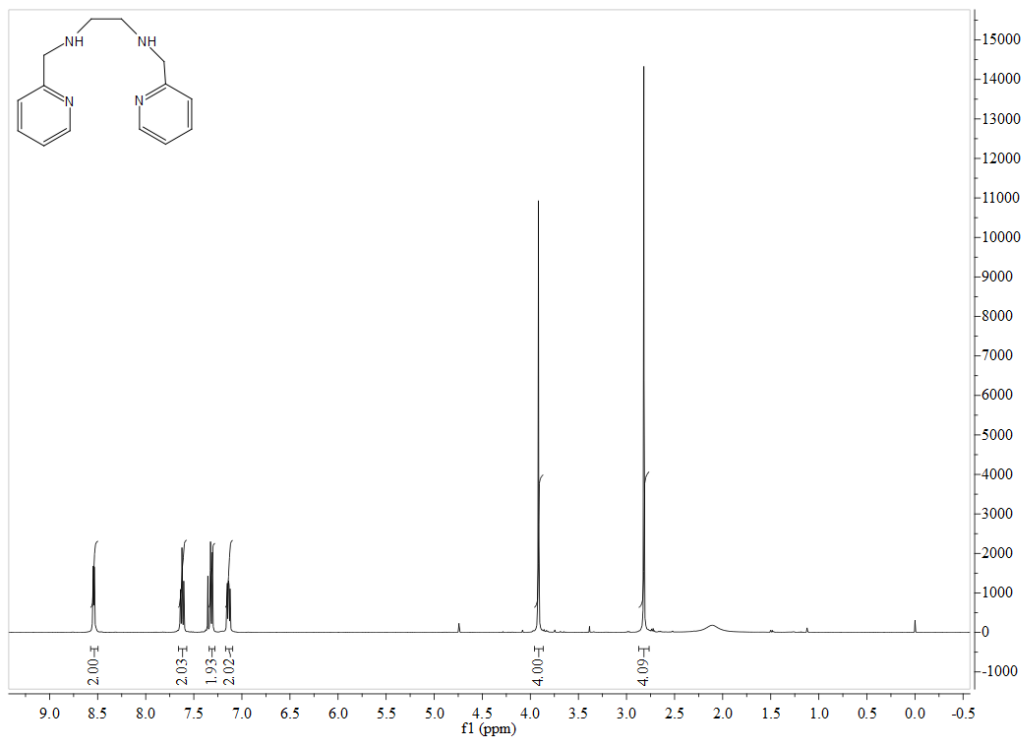


Fig. S4 ¹H NMR spectra of HCMB.

1.3

N,N'-bis(2-hydroxy-5-methyl-3-formylbenzyl)-N,N'-bis-(pyridin-2-ylmethyl)ethylene diamine, H₂L

In a 100 mL round bottom flask, 4.6 g of HCMB (25 mmol) and 3.0 g of pyren (12 mmol) were dissolved in 40 mL of dichloromethane. Then, 3.5 mL of triethylamine (25 mmol) was added dropwise. After 24 h at room temperature, the reaction solution was washed with a saturated solution of NaHCO₃ and the organic layers dried with MgSO₄. After removing the solvent under vacuum, 6.4 g of H₂L were obtained, as viscous yellow oil (96% yield). ¹H NMR (400 MHz, CDCl₃) δ 10.19 (d, *J* = 2.2 Hz, 2H), 8.53 (dd, *J* = 2.8, 2.0 Hz, 2H), 7.59 (dd, *J* = 10.6, 4.7 Hz, 2H), 7.37 (s, 2H), 7.25 (d, *J* = 7.7 Hz, 2H), 7.16 (dd, *J* = 12.7, 7.6 Hz, 4H), 3.74 (s, 4H), 3.66 (s, 4H), 2.75 (s, 4H), 2.23 (s, 6H). ¹³C NMR (100 MHz, CDCl₃) δ 192.6, 159.0, 157.9, 148.9, 137.5, 136.7, 128.8, 128.1, 125.0, 123.2, 122.3, 122.2, 59.4, 54.9, 50.5, 20.3. HRMS (ESI) for C₃₂H₃₅N₄O₄ [M+H⁺]: Calcd: 539.2209; Found: 539.2202. IR (KBr): 2958, 2844, 1590, 1471, 1240, 1083, 989, 871.

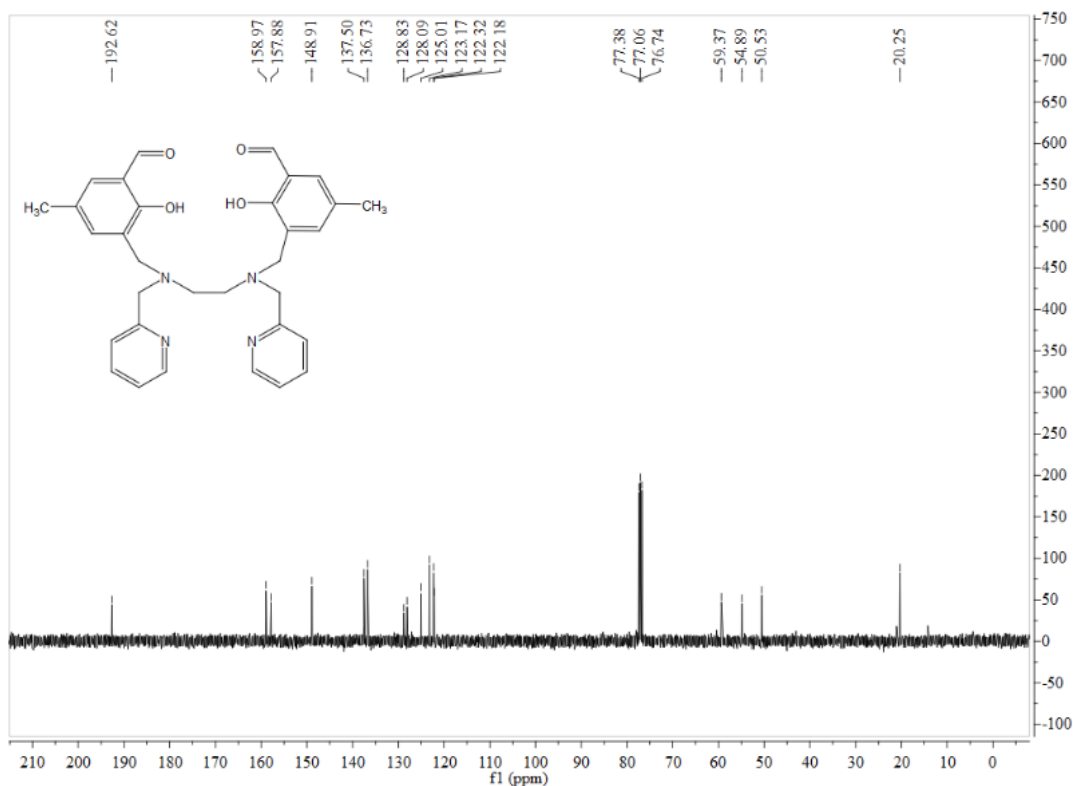


Fig. S5 ¹³C NMR spectra of H₂L.

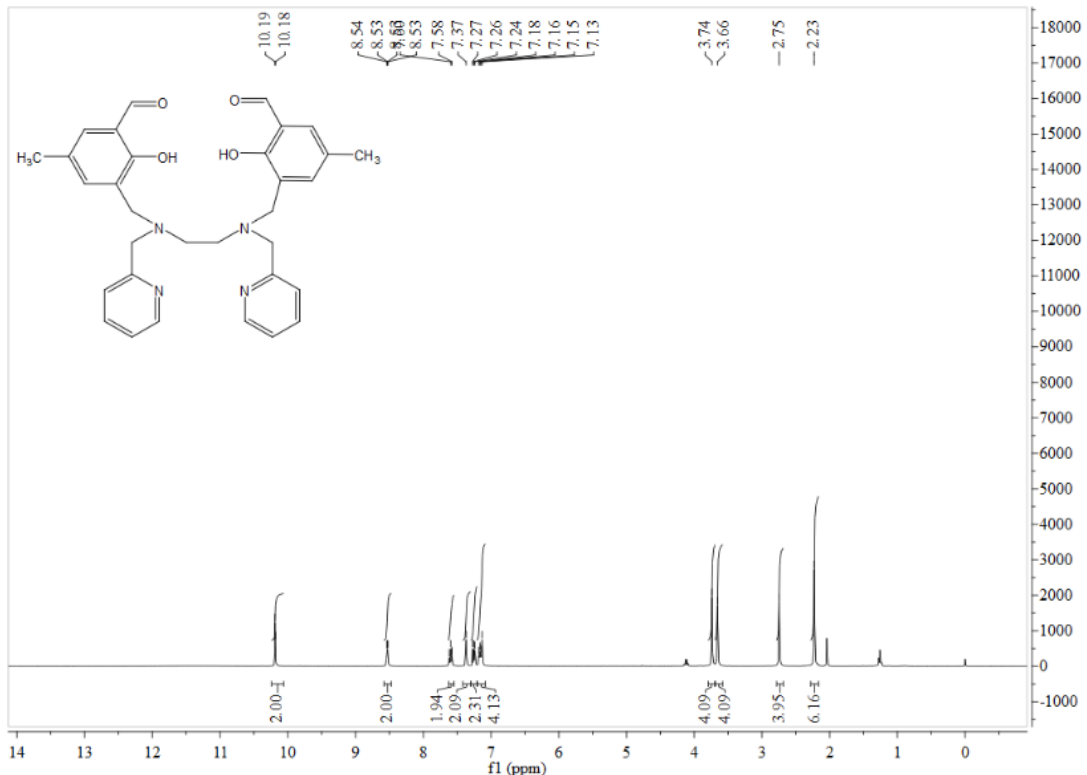


Fig. S6 ¹H NMR spectra of H₂L.

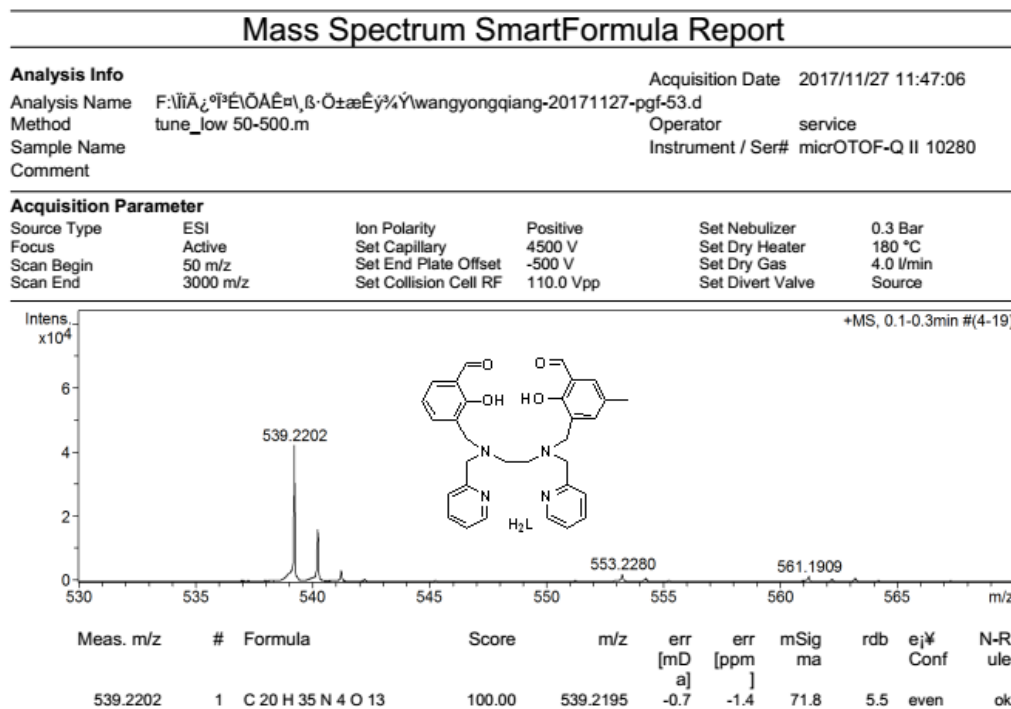


Fig. S7 HRMS spectra of H₂L.

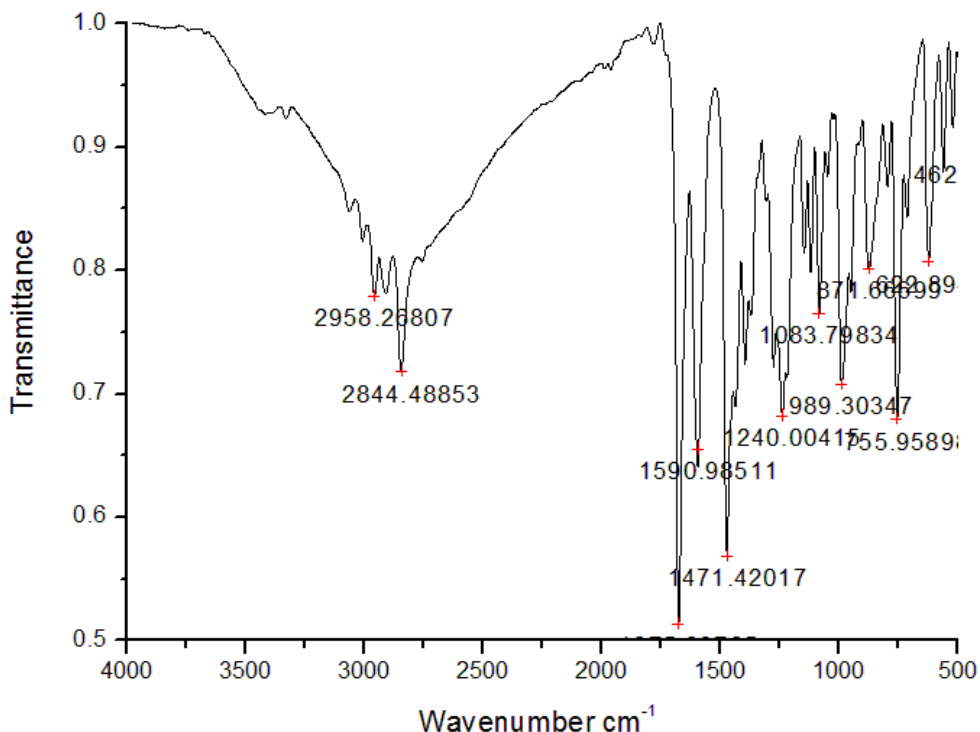


Fig. S8 FTIR spectra of H_2L .

2. The structure information of **1-3, 1a-3a** and **3b**.

Table S1. Crystallographic Data and Structural Refinements for **1a, 2a, 3a** and **3b**.

Compound	1a	2a	3a	3b
molecular formula	C53DyN0.12O13	C51DyN0.25O14	C77H65Dy2N4O10	C65Dy2N17O24
formula weight	1008.78	1002.51	1531.33	1727.82
temperature	293(2)	293(2)	293(2)	293(2)
crystal system	monoclinic	monoclinic	cubic	cubic
space group	<i>C</i> 2/ <i>c</i>	<i>P</i> 2 ₁ / <i>c</i>	<i>P</i> a3	<i>P</i> a3
<i>a</i> (Å)	28.071(2)	22.8242(5)	35.3274(5)	35.3274(5)
<i>b</i> (Å)	14.8132(10)	15.3037(4)	35.3274(5)	35.3274(5)
<i>c</i> (Å)	20.9718(12)	11.8447(3)	35.3274(5)	35.3274(5)
α (deg)	90	90	90	90
β (deg)	96.366(6)	90.236(2)	90	90
γ (deg)	90	90	90	90
<i>V</i> (Å ³)	8666.9(10)	4137.28(16)	44090(2)	43953(2)
<i>Z</i>	8	4	24	24
<i>D</i> _{calc} (g cm ⁻³)	1.546	1.609	1.384	1.562
<i>F</i> (000)	3911	1943	18408	19992
μ/mm^{-1}	9.825	10.305	11.219	11.512

θ min-max/ ^o	3.895-67.246	3.477-67.236	3.064-67.216	3.064-67.216
reflections collected	18385	30251	39571	39571
GOF on F^2	1.029	1.015	0.853	1.036
R_1/wR_2 [$I > 2\sigma(I)$]	0.0710/0.1815	0.0959/0.2397	0.0730/0.1939	0.0935/0.2579
R_1/wR_2 [all data]	0.1115/0.2161	0.1090/0.2545	0.1640/0.2709	0.1915/0.3255

$${}^a R_1 = \sum |F_o| - |F_c| / \sum |F_o|. \quad {}^b wR_2 = [\sum w(F_o^2 - F_c^2)^2 / \sum w(F_o^2)^2]^{1/2}.$$

Table S2. Selected bond lengths (Å) and angles (°) for **1-3**.

Compound 1			
Dy(1)-O(1)	2.223(3)	O(1)-Dy(1)-N(4)	74.93(12)
Dy(1)-O(3)	2.268(3)	O(3)-Dy(1)-N(4)	132.64(12)
Dy(1)-O(6)	2.299(3)	O(6)-Dy(1)-N(4)	113.43(13)
Dy(1)-O(5)	2.334(3)	O(5)-Dy(1)-N(4)	69.68(12)
Dy(1)-N(1)	2.594(4)	N(1)-Dy(1)-N(4)	144.87(12)
Dy(1)-N(4)	2.604(4)	O(1)-Dy(1)-N(2)	76.55(13)
Dy(1)-N(2)	2.626(4)	O(3)-Dy(1)-N(2)	92.62(12)
Dy(1)-N(3)	2.637(4)	O(6)-Dy(1)-N(2)	140.54(12)
O(1)-Dy(1)-O(3)	151.29(12)	O(5)-Dy(1)-N(2)	148.25(12)
O(1)-Dy(1)-O(6)	81.08(12)	N(1)-Dy(1)-N(2)	66.01(12)
O(3)-Dy(1)-O(6)	91.69(13)	N(4)-Dy(1)-N(2)	91.63(12)
O(1)-Dy(1)-O(5)	119.99(12)	O(1)-Dy(1)-N(3)	124.02(12)
O(3)-Dy(1)-O(5)	82.89(12)	O(3)-Dy(1)-N(3)	74.61(12)
O(6)-Dy(1)-O(5)	71.17(11)	O(6)-Dy(1)-N(3)	148.05(12)
O(1)-Dy(1)-N(1)	73.70(12)	O(5)-Dy(1)-N(3)	78.46(12)
O(3)-Dy(1)-N(1)	77.60(12)	N(1)-Dy(1)-N(3)	126.04(13)
O(6)-Dy(1)-N(1)	76.74(12)	N(4)-Dy(1)-N(3)	62.79(12)
O(5)-Dy(1)-N(1)	141.68(12)	N(2)-Dy(1)-N(3)	70.09(12)
Compound 2			
Dy(1)-O(3)	2.219(4)	O(3)-Dy(1)-N(1)	78.17(13)
Dy(1)-O(1)	2.224(4)	O(1)-Dy(1)-N(1)	73.48(13)
Dy(1)-O(5)	2.295(3)	O(5)-Dy(1)-N(1)	77.59(13)
Dy(1)-O(6)	2.302(3)	O(6)-Dy(1)-N(1)	145.41(13)
Dy(1)-N(4)	2.598(4)	N(4)-Dy(1)-N(1)	144.43(13)
Dy(1)-N(1)	2.628(4)	O(3)-Dy(1)-N(2)	94.68(14)
Dy(1)-N(2)	2.648(4)	O(1)-Dy(1)-N(2)	77.03(14)
Dy(1)-N(3)	2.652(4)	O(5)-Dy(1)-N(2)	140.74(13)
O(3)-Dy(1)-O(1)	151.35(13)	O(6)-Dy(1)-N(2)	147.12(13)
O(3)-Dy(1)-O(5)	87.47(13)	N(4)-Dy(1)-N(2)	91.14(14)
O(1)-Dy(1)-O(5)	82.52(13)	N(1)-Dy(1)-N(2)	64.65(14)

O(3)-Dy(1)-O(6)	84.11(13)	O(3)-Dy(1)-N(3)	74.68(13)
O(1)-Dy(1)-O(6)	117.65(13)	O(1)-Dy(1)-N(3)	125.33(13)
O(5)-Dy(1)-O(6)	72.13(12)	O(5)-Dy(1)-N(3)	147.16(13)
O(3)-Dy(1)-N(4)	132.16(13)	O(6)-Dy(1)-N(3)	78.68(13)
O(1)-Dy(1)-N(4)	75.97(13)	N(4)-Dy(1)-N(3)	63.26(14)
O(5)-Dy(1)-N(4)	115.98(13)	N(1)-Dy(1)-N(3)	123.56(14)
O(6)-Dy(1)-N(4)	66.84(12)	N(2)-Dy(1)-N(3)	69.40(14)
Compound 3			
Dy(1)-O(2)	2.300(7)	O(2)-Dy(1)-Dy(2)	156.6(2)
Dy(1)-O(3)	2.304(7)	O(3)-Dy(1)-Dy(2)	88.5(2)
Dy(1)-O(8)	2.310(7)	O(8)-Dy(1)-Dy(2)	31.98(17)
Dy(1)-O(1)	2.319(7)	O(1)-Dy(1)-Dy(2)	113.2(2)
Dy(1)-O(4)	2.336(7)	O(4)-Dy(1)-Dy(2)	111.90(18)
Dy(1)-O(9)	2.370(7)	O(9)-Dy(1)-Dy(2)	32.87(16)
Dy(1)-O(10)	2.449(8)	O(10)-Dy(1)-Dy(2)	81.0(2)
Dy(1)-O(7)	2.480(8)	O(7)-Dy(1)-Dy(2)	82.17(19)
Dy(1)-Dy(2)	3.9031(9)	O(6)-Dy(2)-O(5)	72.7(3)
Dy(2)-O(6)	2.275(8)	O(6)-Dy(2)-O(8)	133.2(3)
Dy(2)-O(5)	2.287(8)	O(5)-Dy(2)-O(8)	83.4(3)
Dy(2)-O(8)	2.297(7)	O(6)-Dy(2)-O(9)	80.5(3)
Dy(2)-O(9)	2.305(7)	O(5)-Dy(2)-O(9)	100.4(3)
Dy(2)-N(2)	2.575(9)	O(8)-Dy(2)-O(9)	64.8(2)
Dy(2)-N(1)	2.585(9)	O(6)-Dy(2)-N(2)	149.3(3)
Dy(2)-N(4)	2.590(11)	O(5)-Dy(2)-N(2)	133.8(3)
Dy(2)-N(3)	2.616(9)	O(8)-Dy(2)-N(2)	73.2(3)
O(2)-Dy(1)-O(3)	114.7(3)	O(9)-Dy(2)-N(2)	104.4(3)
O(2)-Dy(1)-O(8)	142.9(3)	O(6)-Dy(2)-N(1)	122.2(3)
O(3)-Dy(1)-O(8)	82.4(3)	O(5)-Dy(2)-N(1)	76.4(3)
O(2)-Dy(1)-O(1)	73.3(3)	O(8)-Dy(2)-N(1)	88.7(3)
O(3)-Dy(1)-O(1)	73.6(3)	O(9)-Dy(2)-N(1)	153.5(3)
O(8)-Dy(1)-O(1)	81.5(3)	N(2)-Dy(2)-N(1)	64.0(3)
O(2)-Dy(1)-O(4)	79.5(3)	O(6)-Dy(2)-N(4)	69.3(3)
O(3)-Dy(1)-O(4)	73.0(3)	O(5)-Dy(2)-N(4)	104.7(3)
O(8)-Dy(1)-O(4)	137.5(2)	O(8)-Dy(2)-N(4)	157.3(3)
O(1)-Dy(1)-O(4)	121.9(3)	O(9)-Dy(2)-N(4)	132.0(3)
O(2)-Dy(1)-O(9)	146.4(3)	N(2)-Dy(2)-N(4)	86.5(3)
O(3)-Dy(1)-O(9)	83.4(3)	N(1)-Dy(2)-N(4)	73.1(3)
O(8)-Dy(1)-O(9)	63.5(2)	O(6)-Dy(2)-N(3)	81.1(3)
O(1)-Dy(1)-O(9)	140.3(3)	O(5)-Dy(2)-N(3)	153.8(3)
O(4)-Dy(1)-O(9)	79.4(2)	O(8)-Dy(2)-N(3)	116.2(3)
O(2)-Dy(1)-O(10)	81.2(3)	O(9)-Dy(2)-N(3)	75.3(3)
O(3)-Dy(1)-O(10)	144.3(3)	N(2)-Dy(2)-N(3)	71.3(3)
O(8)-Dy(1)-O(10)	104.2(3)	N(1)-Dy(2)-N(3)	118.8(3)

O(1)-Dy(1)-O(10)	141.6(3)	N(4)-Dy(2)-N(3)	64.2(3)
O(4)-Dy(1)-O(10)	79.5(3)	O(6)-Dy(2)-Dy(1)	104.7(2)
O(9)-Dy(1)-O(10)	69.4(3)	O(5)-Dy(2)-Dy(1)	85.2(2)
O(2)-Dy(1)-O(7)	77.9(3)	O(8)-Dy(2)-Dy(1)	32.19(16)
O(3)-Dy(1)-O(7)	140.4(3)	O(9)-Dy(2)-Dy(1)	33.92(17)
O(8)-Dy(1)-O(7)	69.5(2)	N(2)-Dy(2)-Dy(1)	94.2(2)
O(1)-Dy(1)-O(7)	75.0(3)	N(1)-Dy(2)-Dy(1)	120.1(2)
O(4)-Dy(1)-O(7)	145.8(3)	N(4)-Dy(2)-Dy(1)	165.5(2)
O(9)-Dy(1)-O(7)	106.8(3)	N(3)-Dy(2)-Dy(1)	102.3(2)
O(10)-Dy(1)-O(7)	71.9(3)		

Table S3 Dy^{III} ion geometry analysis by SHAPE 2.1 software.

Configuration	ABOXIY, 1	ABOXIY, 2	ABOXIY, 3	
			Dy1	Dy2
Octagon(D8h)	31.594	31.307	31.581	32.874
Heptagonal pyramid(C7v)	21.493	20.923	23.065	23.596
Hexagonal bipyramid(D6h)	12.285	12.168	16.750	12.324
Cube(Oh)	8.272	8.763	9.846	5.044
Square antiprism (D_{4d})	2.401	2.149	0.629	2.679
Triangular dodecahedron (D_{2d})	1.256	1.765	2.480	1.308
Johnson gyrobifastigium J26 (D_{2d})	12.163	11.526	16.448	15.694
Johnson elongated triangular bipyramid J14 (D_{3h})	26.847	26.775	27.866	27.158
Biaugmented trigonal prism J50 (C_{2v})	2.042	1.983	2.874	4.334
Biaugmented trigonal prism (C_{2v})	2.042	2.128	2.248	3.739
Snub sphenoid J84 (D_{2d})	4.272	4.258	5.082	5.166
Triakis tetrahedron(Td)	9.029	9.554	10.699	5.931
Elongated trigonal bipyramid(D3h)	24.373	23.312	24.149	23.932

S H A P E v2.1 Continuous Shape Measures calculation

(c) 2013 Electronic Structure Group, Universitat de Barcelona

Contact: llunell@ub.edu

Dy structures of **1**

OP-8	1 D8h	Octagon
HPY-8	2 C7v	Heptagonal pyramid
HBPY-8	3 D6h	Hexagonal bipyramid
CU-8	4 Oh	Cube
SAPR-8	5 D4d	Square antiprism
TDD-8	6 D2d	Triangular dodecahedron
JGBF-8	7 D2d	Johnson gyrobifastigium J26

JETBPY-8	8 D3h	Johnson elongated triangular bipyramid J14
JBTPR-8	9 C2v	Biaugmented trigonal prism J50
BTPR-8	10 C2v	Biaugmented trigonal prism
JSD-8	11 D2d	Snub diphenoïd J84
TT-8	12 Td	Triakis tetrahedron
ETBPY-8	13 D3h	Elongated trigonal bipyramid

Structure [ML8]	OP-8	HPY-8	HBPY-8	CU-8	SAPR-8
TDD-8	JGBF-8	JETBPY-8	JBTPR-8	BTPR-8	JSD-8
ETBPY-8					TT-8
ABOXIY,	31.594, 26.847,	21.493, 2.042,	12.285, 4.272,	8.272, 9.029,	2.401, 24.373
					1.256, 12.163,

S H A P E v2.1 Continuous Shape Measures calculation
(c) 2013 Electronic Structure Group, Universitat de Barcelona
Contact: llunell@ub.edu

Dy structures of 2

OP-8	1 D8h	Octagon
HPY-8	2 C7v	Heptagonal pyramid
HBPY-8	3 D6h	Hexagonal bipyramid
CU-8	4 Oh	Cube
SAPR-8	5 D4d	Square antiprism
TDD-8	6 D2d	Triangular dodecahedron
JGBF-8	7 D2d	Johnson gyrobifastigium J26
JETBPY-8	8 D3h	Johnson elongated triangular bipyramid J14
JBTPR-8	9 C2v	Biaugmented trigonal prism J50
BTPR-8	10 C2v	Biaugmented trigonal prism
JSD-8	11 D2d	Snub diphenoïd J84
TT-8	12 Td	Triakis tetrahedron
ETBPY-8	13 D3h	Elongated trigonal bipyramid

Structure [ML8]	OP-8	HPY-8	HBPY-8	CU-8	SAPR-8
TDD-8	JGBF-8	JETBPY-8	JBTPR-8	BTPR-8	JSD-8
ETBPY-8					TT-8
ABOXIY,	31.307, 26.775,	20.923, 1.983,	12.168, 4.258,	8.763, 9.554,	2.149, 23.312
					1.765, 11.526,

S H A P E v2.1 Continuous Shape Measures calculation
(c) 2013 Electronic Structure Group, Universitat de Barcelona
Contact: llunell@ub.edu

Dy structures of **3(Dy1)**

OP-8	1 D8h	Octagon
HPY-8	2 C7v	Heptagonal pyramid
HBPY-8	3 D6h	Hexagonal bipyramid
CU-8	4 Oh	Cube
SAPR-8	5 D4d	Square antiprism
TDD-8	6 D2d	Triangular dodecahedron
JGBF-8	7 D2d	Johnson gyrobifastigium J26
JETBPY-8	8 D3h	Johnson elongated triangular bipyramid J14
JBTPR-8	9 C2v	Biaugmented trigonal prism J50
BTPR-8	10 C2v	Biaugmented trigonal prism
JSD-8	11 D2d	Snub diphenoïd J84
TT-8	12 Td	Triakis tetrahedron
ETBPY-8	13 D3h	Elongated trigonal bipyramid

Structure	[ML8]	OP-8	HPY-8	HBPY-8	CU-8	SAPR-8
TDD-8	JGBF-8	JETBPY-8	JBTPR-8	BTPR-8	JSD-8	TT-8
ETBPY-8						
ABOXIY,	31.581,	23.065,	16.750,	9.846,	0.629,	2.480,
27.866,	2.874,	2.248,	5.082,	10.699,	24.149	16.448,

S H A P E v2.1 Continuous Shape Measures calculation

(c) 2013 Electronic Structure Group, Universitat de Barcelona

Contact: llunell@ub.edu

Dy structures of **3(Dy2)**

OP-8	1 D8h	Octagon
HPY-8	2 C7v	Heptagonal pyramid
HBPY-8	3 D6h	Hexagonal bipyramid
CU-8	4 Oh	Cube
SAPR-8	5 D4d	Square antiprism
TDD-8	6 D2d	Triangular dodecahedron
JGBF-8	7 D2d	Johnson gyrobifastigium J26
JETBPY-8	8 D3h	Johnson elongated triangular bipyramid J14
JBTPR-8	9 C2v	Biaugmented trigonal prism J50
BTPR-8	10 C2v	Biaugmented trigonal prism
JSD-8	11 D2d	Snub diphenoïd J84
TT-8	12 Td	Triakis tetrahedron
ETBPY-8	13 D3h	Elongated trigonal bipyramid

Structure	[ML8]	OP-8	HPY-8	HBPY-8	CU-8	SAPR-8
TDD-8	JGBF-8	JETBPY-8	JBTPR-8	BTPR-8	JSD-8	TT-8
ETBPY-8						

ABOXIY , 32.874, 23.596, 12.324, 5.044, 2.679, 1.308,
15.694, 27.158, 4.334, 3.739, 5.166, 5.931, 23.932

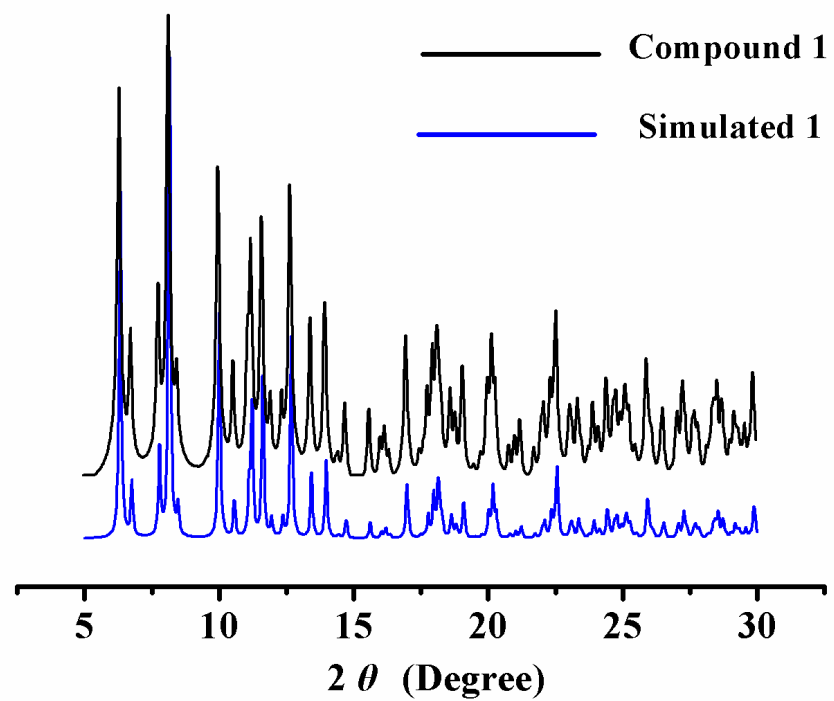


Fig. S9 XRPD curves of **1**.

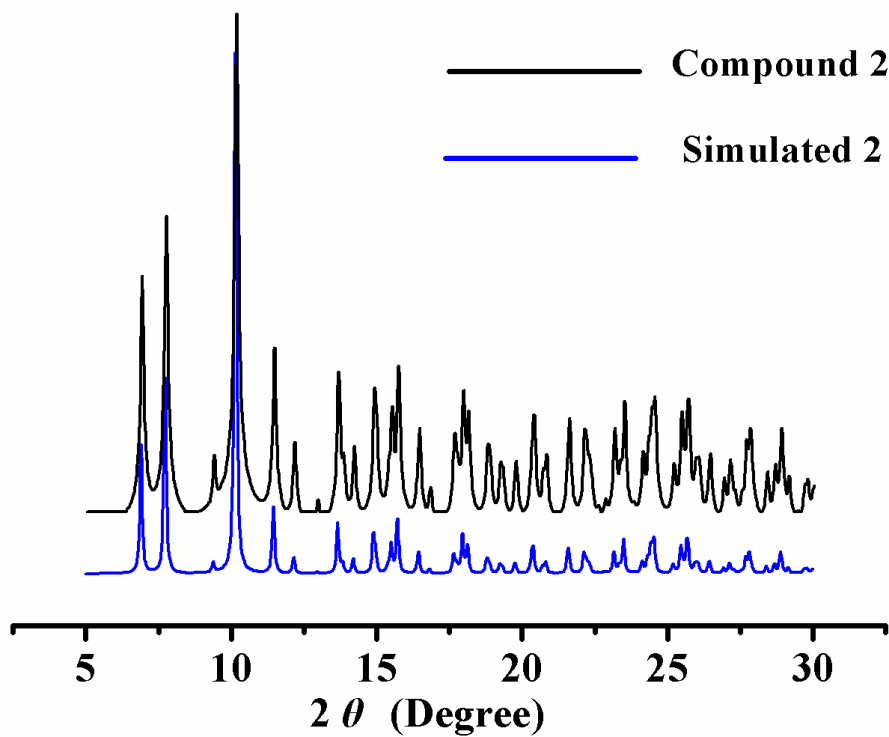


Fig. S10 XRPD curves of **2**.

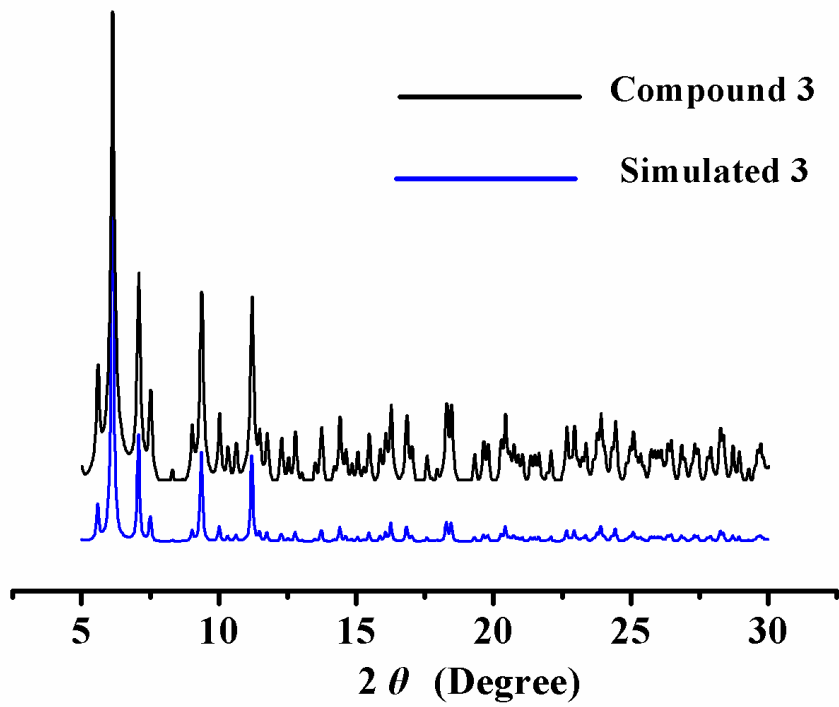


Fig. S11 XRPD curves of **3**.

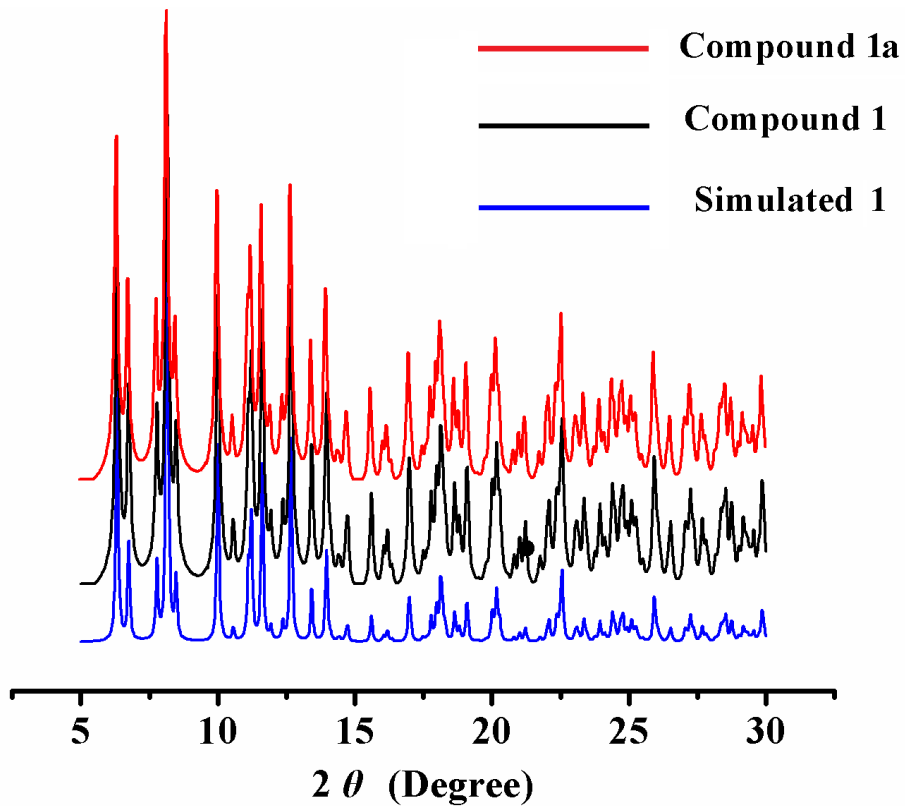


Fig. S12 XRPD curves of **1a**.

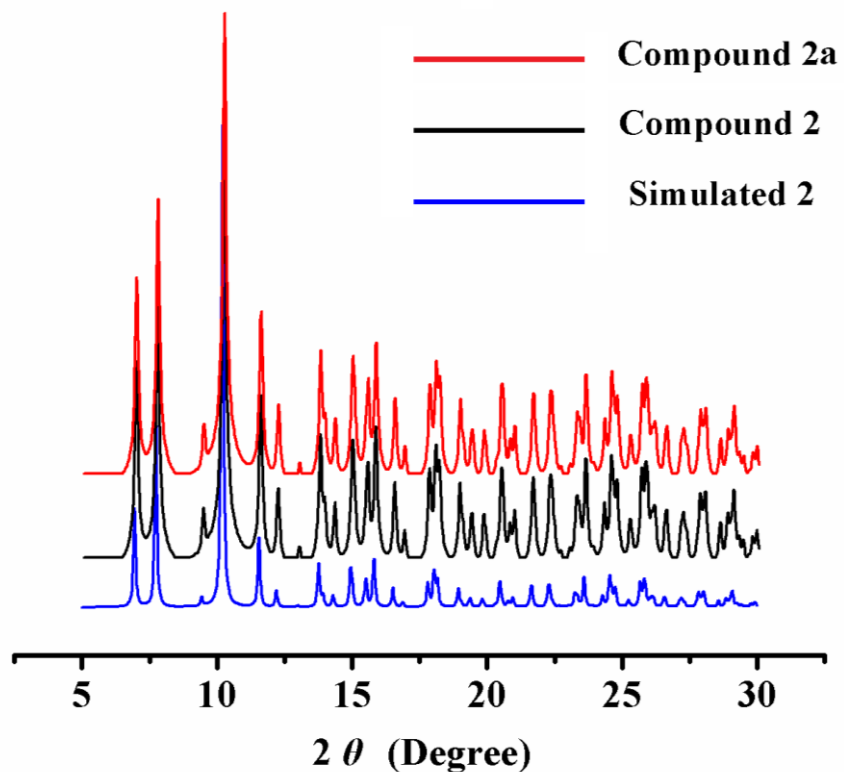


Fig. S13 XRPD curves of **2a**.

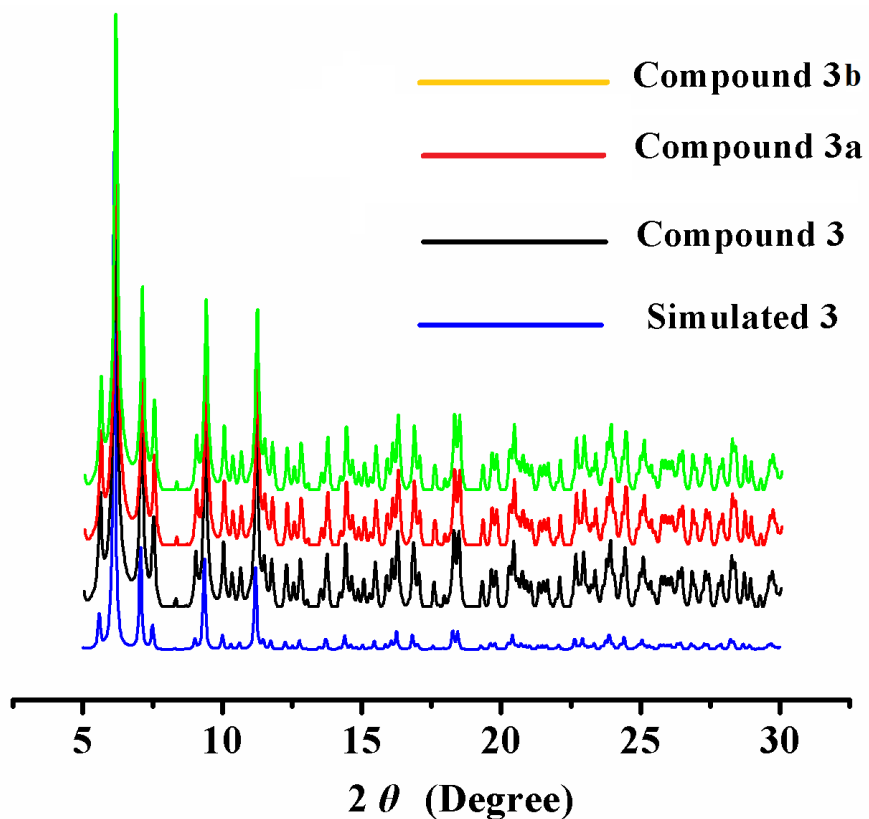


Fig. S12 XRPD curves of **3a** and **3b**.

3. Magnetic hysteresis loop for **1** at 5 K

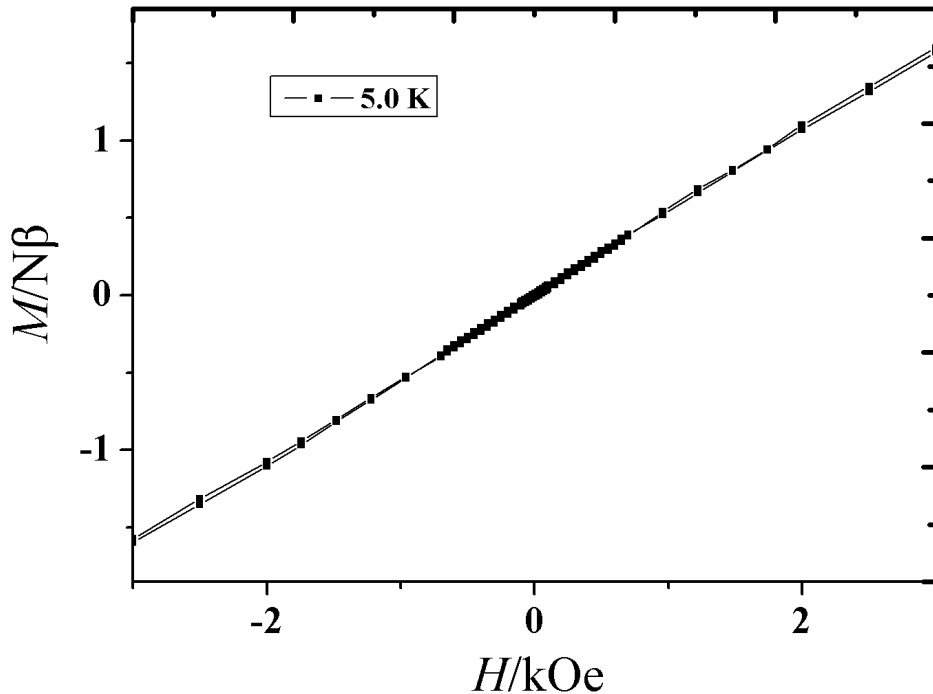


Fig. S15 Magnetic hysteresis loop for **1** at 5 K.

4. Relaxation fitting parameters of **1-3**

The magnetic susceptibility data of **1-3** under a zero dc field were described by the modified Debye functions:

$$\chi'(\omega) = \chi_s + (\chi_t - \chi_s) \frac{1 + (\omega\tau)^{1-\alpha} \sin(\frac{\pi}{2}\alpha)}{1 + 2(\omega\tau)^{1-\alpha} \sin(\frac{\pi}{2}\alpha) + (\omega\tau)^{(2-2\alpha)}}$$

$$\chi''(\omega) = (\chi_t - \chi_s) \frac{(\omega\tau)^{1-\alpha} \cos(\frac{\pi}{2}\alpha)}{1 + 2(\omega\tau)^{1-\alpha} \sin(\frac{\pi}{2}\alpha) + (\omega\tau)^{(2-2\alpha)}}$$

$$\chi''_{\omega=\tau^{-1}} = (\chi_t - \chi_s) \frac{\cos(\frac{\pi}{2}\alpha)}{2 + 2 \sin(\frac{\pi}{2}\alpha)} = \frac{1}{2} (\chi_t - \chi_s) \tan \frac{\pi}{4} (1 - \alpha)$$

Table S4 Relaxation fitting parameters from Least-Squares Fitting of $\chi(\omega)$ data for **1** under a zero applied dc field.

<i>T</i>	$\Delta\chi_1$ (cm ³ mol ⁻¹)	$\Delta\chi_2$ (cm ³ mol ⁻¹)	τ (s)	α
2.0	0.261391E+00	0.361211E+01	0.175656E-02	0.140216E+00
2.2	0.238414E+00	0.327639E+01	0.175393E-02	0.140658E+00
2.4	0.219778E+00	0.299739E+01	0.174849E-02	0.140183E+00
2.6	0.203631E+00	0.275428E+01	0.173895E-02	0.139988E+00
2.8	0.190634E+00	0.256450E+01	0.173304E-02	0.139880E+00
3.0	0.241180E+00	0.320769E+01	0.145563E-02	0.134667E+00
3.2	0.168410E+00	0.224433E+01	0.171481E-02	0.139552E+00
3.6	0.152109E+00	0.199434E+01	0.169600E-02	0.138781E+00
4.0	0.138250E+00	0.179388E+01	0.167278E-02	0.138328E+00
4.4	0.128098E+00	0.163083E+01	0.164985E-02	0.136957E+00
4.8	0.119174E+00	0.149417E+01	0.162239E-02	0.135712E+00
5.2	0.112107E+00	0.137857E+01	0.159383E-02	0.133974E+00
5.6	0.104950E+00	0.128026E+01	0.156388E-02	0.133034E+00
6.0	0.989626E-01	0.119526E+01	0.153371E-02	0.132015E+00
6.5	0.931221E-01	0.110274E+01	0.149254E-02	0.129260E+00
7.0	0.879650E-01	0.102420E+01	0.145102E-02	0.126618E+00
7.5	0.832263E-01	0.955982E+00	0.140595E-02	0.123585E+00
8.0	0.786051E-01	0.896620E+00	0.135879E-02	0.122136E+00
9.0	0.719128E-01	0.797233E+00	0.126102E-02	0.115251E+00
10	0.662030E-01	0.718566E+00	0.115962E-02	0.108454E+00
11	0.617714E-01	0.652911E+00	0.105188E-02	0.100305E+00
12	0.576881E-01	0.599437E+00	0.943958E-03	0.930296E-01
14	0.502664E-01	0.514226E+00	0.728314E-03	0.778799E-01
16	0.439224E-01	0.452475E+00	0.538635E-03	0.686484E-01
18	0.378291E-01	0.404149E+00	0.377124E-03	0.676439E-01
20	0.333472E-01	0.365050E+00	0.245487E-03	0.735590E-01
25	0.346309E-01	0.294894E+00	0.526036E-04	0.106273E+00
30	0.149166E-06	0.248538E+00	0.702782E-05	0.428005E-01

Table S5 Relaxation fitting parameters from Least-Squares Fitting of $\chi(\omega)$ data for **2** under a zero applied dc field.

<i>T</i>	$\Delta\chi_1$ (cm ³ mol ⁻¹)	$\Delta\chi_2$ (cm ³ mol ⁻¹)	τ (s)	α
2.0	0.465942E-01	0.289863E+01	0.197708E-01	0.215831E+00
2.2	0.425992E-01	0.263810E+01	0.198260E-01	0.216843E+00
2.4	0.394299E-01	0.242025E+01	0.198487E-01	0.216996E+00
2.6	0.366161E-01	0.223006E+01	0.198124E-01	0.218369E+00
2.8	0.340803E-01	0.207884E+01	0.198187E-01	0.219241E+00
3.0	0.348816E-01	0.209333E+01	0.196503E-01	0.219665E+00
3.4	0.286720E-01	0.171768E+01	0.195513E-01	0.221349E+00
3.8	0.261757E-01	0.154193E+01	0.193488E-01	0.222135E+00

4.2	0.248469E-01	0.139581E+01	0.189757E-01	0.220758E+00
4.6	0.232428E-01	0.127673E+01	0.186536E-01	0.220674E+00
5.0	0.225191E-01	0.117522E+01	0.182546E-01	0.219616E+00
6.0	0.210690E-01	0.980746E+00	0.171252E-01	0.212692E+00
7.0	0.206185E-01	0.838673E+00	0.157228E-01	0.202344E+00
8.0	0.198936E-01	0.731708E+00	0.142334E-01	0.188511E+00
9.0	0.192121E-01	0.649344E+00	0.127696E-01	0.176043E+00
10	0.186252E-01	0.581887E+00	0.112805E-01	0.161074E+00
12	0.155628E-01	0.482084E+00	0.855062E-02	0.136948E+00
14	0.132252E-01	0.411135E+00	0.632224E-02	0.116947E+00
16	0.948164E-02	0.359856E+00	0.456981E-02	0.104106E+00
18	0.921472E-02	0.320504E+00	0.320975E-02	0.982376E-01
20	0.868805E-02	0.288662E+00	0.216889E-02	0.969097E-01
22	0.847249E-02	0.261811E+00	0.139808E-02	0.761193E-01
24	0.806337E-02	0.239134E+00	0.790216E-03	0.811517E-01
26	0.788403E-02	0.221633E+00	0.381680E-03	0.841454E-01
28	0.768594E-02	0.208025E+00	0.171161E-03	0.806470E-01
30	0.752449E-02	0.194947E+00	0.844968E-04	0.826842E-01
35	0.717969E-02	0.167564E+00	0.441949E-04	0.783574E-01

Table S6 Relaxation fitting parameters from Least-Squares Fitting of $\chi(\omega)$ data for **3** under a zero applied dc field.

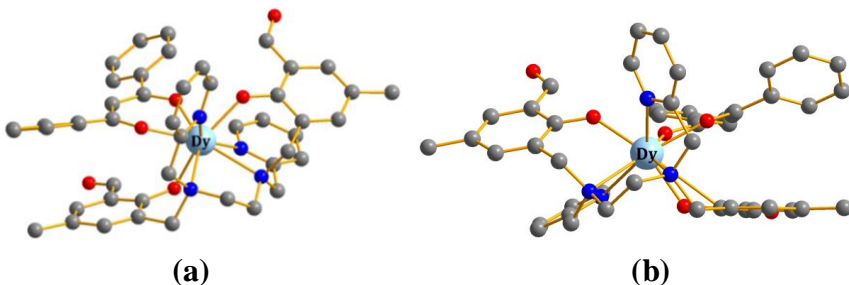
T	$\Delta\chi_1$ (cm ³ mol ⁻¹)	$\Delta\chi_2$ (cm ³ mol ⁻¹)	τ (s)	α
2.0	0.121077E+01	0.673671E+01	0.796071E-03	0.397530E+00
2.2	0.109801E+01	0.607124E+01	0.756133E-03	0.399594E+00
2.4	0.996063E+00	0.552736E+01	0.718862E-03	0.401859E+00
2.6	0.914338E+00	0.505993E+01	0.688912E-03	0.403261E+00
2.8	0.855042E+00	0.468149E+01	0.668629E-03	0.404206E+00
3.0	0.860441E+00	0.439862E+01	0.821137E-03	0.413667E+00
3.2	0.745063E+00	0.407136E+01	0.626539E-03	0.407282E+00
3.4	0.700888E+00	0.382056E+01	0.609033E-03	0.408323E+00
3.6	0.662317E+00	0.359830E+01	0.591768E-03	0.409957E+00
3.8	0.648599E+00	0.339939E+01	0.587118E-03	0.409511E+00
4.0	0.623371E+00	0.322213E+01	0.574380E-03	0.411000E+00
4.2	0.600968E+00	0.306109E+01	0.559941E-03	0.411077E+00
4.4	0.568168E+00	0.292034E+01	0.542438E-03	0.414651E+00
4.6	0.554784E+00	0.278905E+01	0.533813E-03	0.415430E+00
4.8	0.545100E+00	0.266777E+01	0.525098E-03	0.415851E+00
5.0	0.540499E+00	0.255663E+01	0.520293E-03	0.415488E+00
5.5	0.531911E+00	0.231441E+01	0.507471E-03	0.413589E+00
6.0	0.536898E+00	0.211610E+01	0.505842E-03	0.409592E+00
6.5	0.554169E+00	0.194685E+01	0.513723E-03	0.400435E+00
7.0	0.571697E+00	0.180202E+01	0.523581E-03	0.387980E+00

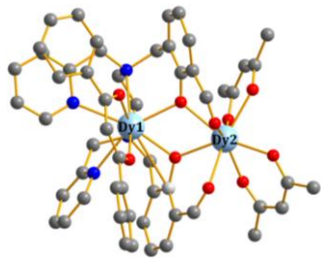
8.0	0.594646E+00	0.156763E+01	0.521257E-03	0.352869E+00
10	0.578048E+00	0.124204E+01	0.341513E-03	0.274351E+00

5. Computational details

For compounds **1** and **2**, there is only one magnetic center Dy^{III} ion. For binuclear compound **3**, it has two types of Dy^{III} fragments, and thus two Dy^{III} fragments were calculated. Complete-active-space self-consistent field (CASSCF) calculations on compounds **1-3** (seen Fig. S8 for the calculated complete structures of compounds **1** and **2**, and the model structure of compound **3**) extracted from the compounds on the basis of single-crystal X-ray determined geometry have been carried out with MOLCAS 8.2^{S1} program package. For compound **3**, each Dy^{III} fragment was calculated keeping the experimentally determined structure of the corresponding compound while replacing the neighbouring Dy^{III} ion by diamagnetic Lu^{III}.

The basis sets for all atoms are atomic natural orbitals from the MOLCAS ANO-RCC library: ANO-RCC-VTZP for Dy^{III} ion; VTZ for close N and O; VDZ for distant atoms. The calculations employed the second order Douglas-Kroll-Hess Hamiltonian, where scalar relativistic contractions were taken into account in the basis set and the spin-orbit couplings were handled separately in the restricted active space state interaction (RASSI-SO) procedure. For individual Dy^{III} fragment, active electrons in 7 active spaces include all *f* electrons (CAS(9 in 7)) in the CASSCF calculation. To exclude all the doubts, we calculated all the roots in the active space. We have mixed the maximum number of spin-free state which was possible with our hardware (all from 21 sextets, 128 from 224 quadruplets, 130 from 490 doublets). SINGLE-ANISO^{S2} program was used to obtain the energy levels, *g* tensors, *m_J* values, magnetic axes, *et al.*, based on the above CASSCF/RASSI-SO calculations.





(c)

Fig. S16 Calculated structures of compounds **1-3** (a-c); H atoms are omitted.

To fit the exchange interaction in compound **3**, we took two steps to obtain them. Firstly, we calculated individual Dy^{III} fragments using CASSCF to obtain the corresponding magnetic properties. Then, the exchange interaction between the magnetic centers is considered within the Lines model,^{S3} while the account of the dipole-dipole magnetic coupling is treated exactly. The Lines model is effective and has been successfully used widely in the research field of *f*-element single-molecule magnets.^{S4}

For compound **3**, there is only one type of J .

The exchange Ising Hamiltonian is:

$$H_{exch} = -J_1 \hat{S}_{Dy1}^z \hat{S}_{Dy2}^z \quad (S1)$$

The J_{total} is the parameter of the total magnetic interaction ($J_{total} = J_{dipolar} + J_{exchange}$)

between magnetic center ions. The $\hat{S}_{Dy}^z = \pm 1/2$ are the ground pseudospin on the Dy^{III} sites. The dipolar magnetic coupling can be calculated exactly, while the exchange coupling constants were fitted through comparison of the computed and measured magnetic susceptibility using the Poly_Aniso program.^{S2}.

Table S7 Exchange energies (cm^{-1}) and main values of the g_z for the lowest two exchange doublets of compound **3**.

	3	
	E/cm^{-1}	g_z
Dy1	0.0	33.718
Dy2	0.5	17.959

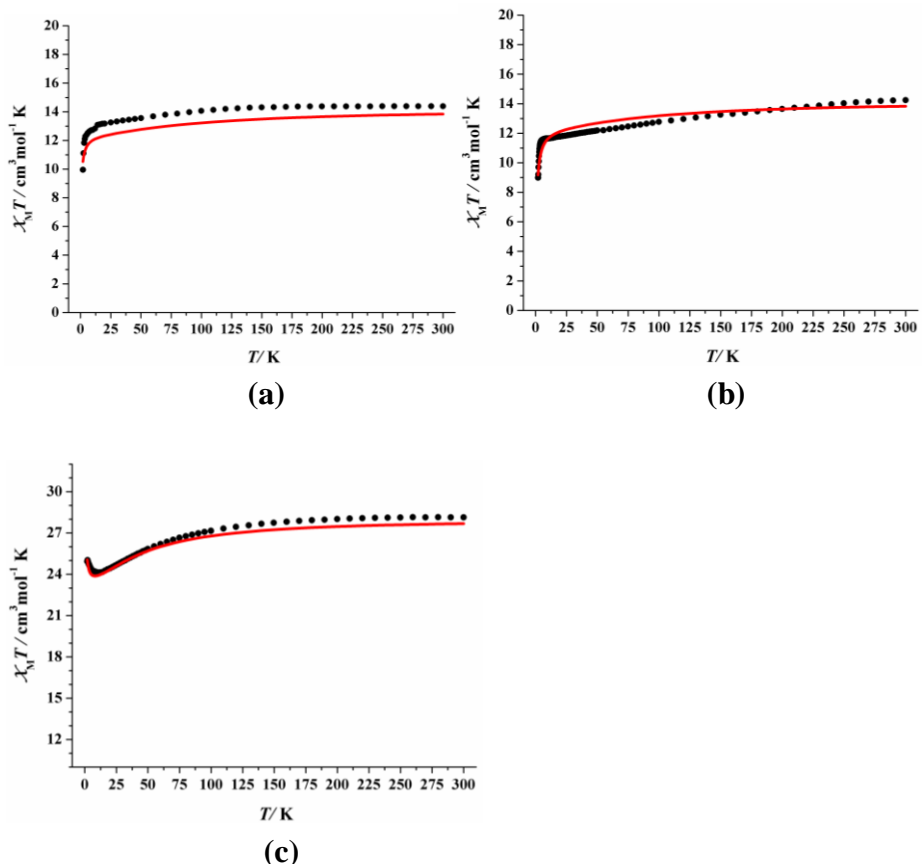


Fig. S17 Calculated (red solid line) and experimental (black circle dot) data of magnetic susceptibilities of compounds **1-3** (a-c). The intermolecular interactions zJ' of **1-3** were fitted to -0.10 , -0.08 and -0.00 cm^{-1} , respectively.

References:

- S1 F. Aquilante, J. Autschbach, R. K. Carlson, L. F. Chibotaru, M. G. Delcey, L. De Vico, I. Fdez. Galván, N. Ferré, L. M. Frutos, L. Gagliardi, M. Garavelli, A. Giussani, C. E. Hoyer, G. Li Manni, H. Lischka, D. Ma, P. Å. Malmqvist, T. Müller, A. Nenov, M. Olivucci, T. B. Pedersen, D. Peng, F. Plasser, B. Pritchard, M. Reiher, I. Rivalta, I. Schapiro, J. Segarra-Martí, M. Stenrup, D. G. Truhlar, L. Ungur, A. Valentini, S. Vancoillie, V. Veryazov, V. P. Vysotskiy, O. Weingart, F. Zapata, R. Lindh, MOLCAS 8: New Capabilities for Multiconfigurational Quantum Chemical Calculations across the Periodic Table, *J. Comput. Chem.*, **2016**, *37*, 506.
- S2 (a) Chibotaru, L. F.; Ungur, L.; Soncini, A. *Angew. Chem. Int. Ed.*, **2008**, *47*, 4126.
 (b) Ungur, L.; Van den Heuvel, W.; Chibotaru, L. F. *New J. Chem.*, **2009**, *33*, 1224.
 (c) Chibotaru, L. F.; Ungur, L.; Aronica, C.; Elmoll, H.; Pilet, G.; Luneau, D. *J. Am. Chem. Soc.*, **2008**, *130*, 12445.
- S3 Lines, M. E. *J. Chem. Phys.* **1971**, *55*, 2977.
- S4 (a) Mondal, K. C.; Sundt, A.; Lan, Y. H.; Kostakis, G. E.; Waldmann, O.; Ungur, L.; Chibotaru, L. F.; Anson, C. E.; Powell, A. K. *Angew. Chem. Int. Ed.* **2012**, *51*, 7550. (b) Langley, S. K.; Wielechowski, D. P.; Vieru, V.; Chilton, N. F.; Moubaraki, B.; Abrahams, B. F.; Chibotaru, L. F.; Murray, K. S. *Angew. Chem. Int.*

Ed. **2013**, 52, 12014.